Filamentous cheater phages drive bacterial and phage populations to lower fitness

Nanami Kubota[1], Michelle R. Scribner[1], and Vaughn S. Cooper[1,2,3,*]

[1]Department of Microbiology and Molecular Genetics, School of Medicine, University of Pittsburgh, Pittsburgh, Pennsylvania, USA

[2]Center for Evolutionary Biology and Medicine, University of Pittsburgh, Pittsburgh, Pennsylvania, USA

[3]Lead contact

*Correspondence: vaughn.cooper@pitt.edu

Summary

Many bacteria carry phage genome(s) in their chromosome (i.e., prophage), and this intertwines the fitness of the bacterium and the phage. Most *Pseudomonas aeruginosa* strains carry filamentous phages called Pf that establish chronic infections and do not require host lysis to spread. However, spontaneous mutations in the Pf repressor gene (*pf5r*) can allow extreme phage production that slows bacterial growth and increases cell death, violating an apparent détente between bacterium and phage. We observed this paradoxical outcome in an evolution experiment with *P. aeruginosa* in media simulating nutrients from the cystic fibrosis airway. Bacteria containing *pf5r* mutant phage grow to a lower density but directly outcompete their ancestor and convert them into *pf5r* mutants via phage superinfection. Reduced fitness therefore spreads throughout the bacterial population, driven by weaponized Pf. Yet high intracellular phage replication facilitates another evolutionary conflict: “cheater miniphages” lacking capsid genes invade populations of full-length phages within cells. Although bacteria containing both full-length phages and miniphages are most immune to superinfection by limiting the Pf receptor, this hybrid vigor is extremely unstable, as a classic Tragedy of the Commons scenario ensues that results in complete prophage loss. The entire cycle – from phage hyperactivation to miniphage invasion to prophage loss – can occur within 24h, showcasing rapid coevolution between bacteria and their filamentous phages. This study demonstrates that *P. aeruginosa*, and potentially many other bacterial species that carry filamentous prophages, risk being exploited by these phages in a runaway process that reduces fitness of both host and virus.

Keywords

Pseudomonas aeruginosa, filamentous phage, Inoviridae, cheating, Tragedy of the Commons, experimental evolution, lysogeny, Pf phage, intracellular competition

Introduction

Many bacteria carry genetic parasites such as lysogenized phages, and a fundamental question is how the presence of these genetic parasites affects the evolutionary trajectory of both the bacterial host and phage. Temperate phages that are integrated into their bacterial host chromosome (prophages) have their fitness tied to their host, and likewise, the host phenotype and fitness are also influenced by the presence of prophage.[1–4] While prophages may encode beneficial traits for the bacteria, such as antibiotic resistance genes[5,6] or superinfection exclusion mechanisms[7], maintenance of an active prophage comes with costs such as the potential for cell lysis.[6] Filamentous phages belonging to the *Inoviridae* family are unique from other phages because they do not require host cell lysis to produce progeny.[8,9] This lowers the risk to the host to maintain an active prophage. Since phage activation and replication do not necessarily kill the host, filamentous phage can achieve increased population size, experience more mutations, and develop greater diversity. Consequently, seemingly clonal bacterial cells may differ in the genetic and phenotypic composition of their phage populations, broadening heterogeneity and the number of traits that selection may act upon.

Many *Pseudomonas aeruginosa* strains carry filamentous Pf prophage or Pf phage-like elements in their chromosome[10], including common laboratory strains like PAO1 with its Pf4 prophage and UCBPP-PA14 (shortened as PA14) with its Pf5 prophage.[11] *P. aeruginosa* is a Gram-negative opportunistic pathogen that causes many hospital-acquired infections and is the major infectious threat for persons with cystic fibrosis (CF). As of 2022, approximately 26.0% of people in the CF Foundation Patient Registry tested positive for *P. aeruginosa* with that percentage increasing to 59.5% in those who met the criteria for Advanced Lung Disease.[12] As CF patients age, their infecting *P. aeruginosa* isolates are more likely to carry Pf prophage.[10] This association may be driven by functions provided by Pf phages to their bacterial host during infection, as their negatively charged filaments can make biofilms more robust, which delays wound healing and protects bacteria from antibiotics.[3,10,13–15] Consequently there are both fundamental and clinical needs to understand ecological and evolutionary interactions between Pf and their host bacteria.

In a previous evolution experiment with *P. aeruginosa* PA14 grown in media containing nutrients found in CF lung environments, we observed this nutritional environment was sufficient to select for clinically relevant bacterial phenotypes.[16] Within one evolved population, we discovered mutations in the Pf5 phage repressor (*pf5r*) gene within the Pf5 prophage genome that rose to high frequency, which motivated this study. We learned that the *pf5r* mutation converts Pf5 phage into a "superinfective" form with increased intracellular phage replication and Pf5 phage production. However, these cells grew significantly slower than those with wildtype (WT) Pf5, posing a puzzle of how the *pf5r* mutation rose to high frequency. We show that PA14 *pf5r* mutants outcompete their ancestor by weaponizing their *pf5r* mutant phage, and we provide evidence of how this imposes a greater cost on the newly superinfected victim cell than on the *pf5r* phage donor cell. Paradoxically, this dynamic progressively reduces bacterial population fitness. Yet these selfish superinfective phage themselves become victimized by cheater "miniphages" lacking structural genes, resolving rapidly in a phage Tragedy of the Commons that resets the entire system. The robust conditions of this experimental model indicate the potential for rapid coevolution between bacteria and filamentous phage in *P. aeruginosa,* as well as in other bacteria carrying inoviruses, affecting a range of traits essential for fitness.

Results

Defective Pf phage repressor leads to runaway Pf replication and increased intracellular phage diversity

Mutations that disrupt the prophage repressor gene can trigger phage activation, leading to the emergence of hyper-replicative Pf phage.[17–19] In a previous evolution experiment begun with a clone of *P. aeruginosa* PA14 analyzed by longitudinal whole-population genome sequencing[16,20], we noticed increased sequencing coverage, or read depth, along the Pf5 prophage region in one evolved population (Supp. Fig 1). Further investigation of sequencing results showed a 16bp duplication mutation within the Pf5 phage repressor gene (*pf5r*) and circularization of the Pf5 genome, indicating active Pf5 phage (Supp. Table 1). The *pf5r* gene is within the prophage region that is integrated into the bacterial chromosome, and so we denote bacteria and phage genotypes with the *pf5r* mutation using an asterisk (e.g., PA14* and Pf5*, respectively, see Table 1 for additional nomenclature). To isolate the *pf5r* mutation in a clean genomic background, we attempted to infect PA14 wildtype (WT) with the Pf5* phage from the

102 evolution experiment, and were successful (see Methods for more detail). The isolated clone
103 (PA14*full) also showed higher read depth across the prophage region (Fig 1B) relative to PA14
104 WT (Fig 1A) and to the surrounding genome, demonstrating that the *pf5r* mutation is
105 responsible for the phage activation and that this trait can be horizontally transferred.
106 Sequencing data also supported excision and circularization of the prophage genome, indicating
107 prophage induction (Supp Table 1). In summary, Pf5* prophage undergo increased replication
108 and enable phage-encoded traits to be horizontally spread by superinfecting neighboring cells
109 that have wildtype Pf5 prophage.
110
111 **Cheater miniphages evolve following increased intracellular phage population from**
112 **defective Pf repressor**
113 Defective Pf repressor genes have been associated with increased numbers of
114 intracellular Pf phage, which increases the potential for the evolution of genetically diverse
115 phage.[19] Whole genome sequencing (WGS) of the newly isolated PA14*full showed increased
116 copy numbers of both WT and mutated *pf5r* genes, indicating that both mutant and endogenous
117 phage replication are upregulated (Supp. Table 1). Notably, in addition to the *pf5r*
118 polymorphism, the genome lengths of Pf5 varied. Some PA14* isolates only carried full-length
119 phages (i.e. PA14*full), others contained a mix of both full-length and smaller phage genomes
120 (i.e. PA14*full/mini), and some bacterial clones only contained smaller phage genomes
121 (PA14*mini). These smaller phage genomes, termed “miniphage,” have large deletions of
122 multiple structural genes encoding capsid proteins (Fig 1C&D and Supp. Fig. 2). We observed
123 the emergence of miniphage multiple times among PA14* lineages and even within the same
124 bacterial clone, where the deletion lengths varied despite affecting the same structural genes
125 (Supp. Fig. 3). This high degree of parallelism indicates strong selection for these reduced
126 phage genomes.
127 Miniphages can be considered cheaters because they do not produce structural phage
128 proteins like capsid, which are public goods usable by any replicating phage. Under intense
129 intracellular phage competition, phages with smaller genome sizes can potentially replicate
130 faster than full-length phages and use such public resources to promote selfish replication.
131 Taken together, we observed that the emergence of the defective Pf repressor quickly leads to
132 extreme levels of Pf reproduction, resulting in increased intracellular phage diversity and
133 genome degradation due to intracellular phage competition.
134

135 **Pf repressor bacterial mutants release hyper-replicative phage that increase mutant**
136 **fitness but lower population fitness**
137 Filamentous phages uniquely do not require host cell lysis to reproduce and
138 propagate.[8,9] However, superinfective Pf4 phages have been linked to an autolysis phenotype in
139 *P. aeruginosa* and can kill their bacterial host.[21,22] To determine whether bacterial hosts
140 containing different combinations of Pf5* genotypes were negatively affected by excess phage
141 production, we compared their growth rates in isolation. The PA14* genotype grew significantly
142 worse than WT, indicating high phage production was costly (Fig 2A&B and Supp Fig 4). Given
143 the extreme cost of hyper-replicative Pf5, it seems paradoxical that defective Pf5r would be
144 favored during experimental evolution of PA14 populations maintained in large populations
145 (>10^7 cells) with efficient selection. We considered two non-mutually exclusive hypotheses: (1)
146 the phage benefits from the defective repressor by increasing its replication rate, which enables
147 horizontal spread in the bacterial population by superinfection, and/or (2) the bacterium benefits
148 from Pf5r mutant phage by being able to outcompete bacteria lacking them. We were able to
149 horizontally transfer Pf5* phage into PA14 WT, so the former scenario is possible. However,
150 PA14* also outcompeted the PA14 WT in direct competition (Fig 2C and Fig 4B), indicating that
151 bacteria currently infected with Pf5* phage pay a lower cost for this infection than naïve cells.
152 This demonstrates that PA14* bacteria benefit from producing hyper-replicative Pf5 phage in
153 direct competition with uninfected cells despite paying costs of reduced growth rates and yield.
154 We next tested whether the phages themselves, and not other physiological changes to
155 PA14* induced by the phage, were responsible for suppressing PA14 WT growth. However,
156 unlike Pf4 phage in PAO1, Pf5 phages do not form plaques on PA14 so we are unable to
157 quantify phage via plaque assays. Instead, we tested whether phage-containing filtered
158 supernatant from superinfected strains could inhibit WT growth as seen in direct competition.
159 Supernatants of both PA14*full and PA14*full/mini suppressed WT growth but WT supernatant
160 did not (Fig 3A). We repeated these supernatant experiments with PA14Δ*pilA*, which does not
161 produce the phage receptor type IV pilus (TFP) and should be immune to superinfection, and
162 found no growth defect (Fig 4A). Finally, we competed PA14Δ*pilA* directly against PA14*full and
163 PA14*full/mini and found the immune TFP mutant outcompeted both superinfected strains (Fig
164 4B). These results further support the hypothesis that PA14*full and PA14*full/mini each
165 suppress PA14 WT growth via Pf5* production. The fitness superiority of the TFP mutant that is
166 immune to Pf5 superinfection shows that PA14* pays a cost for hyper-producing Pf5* phage,
167 but the cost of Pf5* infection is greater to naïve PA14 WT than to PA14* (Fig 2C).
168

169 **Bacteria with both hyper-replicative full-length phage and miniphage survive**
170 **superinfection by downregulating the phage receptor**
171 How PA14* seemingly tolerates Pf5* phage infection better than newly infected WT is
172 unclear. Further, the PA14*full/mini genotype outcompetes WT better than PA14*full, despite
173 both producing high levels of Pf5. We hypothesized that PA14*full/mini can better survive in the
174 presence of Pf5* phage because this genotype can downregulate TFP function better than
175 PA14*full, thereby becoming more phage-resistant. To measure TFP function, we assayed the
176 extent of bacterial twitching motility, known to be mediated by TFP[23,24], as a proxy. Indeed, both
177 superinfected genotypes show reduced twitching, but PA14*full/mini is even less motile,
178 indicating improved immunity to external Pf5* phage (Fig 3B). This ability to downregulate TFP
179 to a greater extent provides an explanation for the greater fitness of the bacterium containing a
180 mixture of full-length and miniphage relative to WT.
181 As noted previously, we observed multiple independent origins of miniphages in cells
182 with defective Pf repressor genes, but remarkably the deletion boundaries differed by only a few
183 nucleotides (Supp. Fig. 2). Each miniphage lost not only genes encoding structural proteins but
184 also the *pfsE* gene encoding a superinfection exclusion protein (PA0721 in PAO1 and
185 PA14_48960 in PA14).[7,25] Many temperate phages encode superinfection exclusion
186 mechanisms to protect their host from other phages and to decrease phage intracellular
187 competition.[26,27] PfsE prevents superinfection by binding to PilC in TFP, which prevents pilus
188 extension and stops phages like Pf from binding to TFP.[7] For miniphages lacking structural
189 genes like capsid, losing PfsE allows their host to become superinfected with “cooperative” full-
190 length Pf phage, thereby rescuing the miniphage from being nonfunctional or lost. However,
191 *pfsE* loss generates two new levels of conflict: first, between miniphage and full-length Pf phage
192 by increasing phage intracellular competition via superinfection, and second, between
193 miniphage and the bacterial host by increasing vulnerability of the bacterial host to other
194 phages. Recurrent miniphage evolution clearly destabilizes the balance of fitness between Pf
195 and their bacterial hosts.
196
197 **Bacteria with defective Pf repressor can rapidly lose Pf prophage due to intracellular**
198 **phage competition.**
199 Rampant phage replication causes acute competition for host resources and public
200 goods involved in replication. Consequently, cheater miniphages that do not produce capsid
201 proteins experience increased fitness at the expense of cooperative, full-length phages. WGS of
202 PA14* revealed that the intracellular phage population in a single bacterial colony can be

203 remarkably diverse, with some cells carrying different mixtures of Pf5 WT, Pf5*full, and Pf5*mini
204 phages including multiple genotypes within each phage class. Miniphage genotypes rose
205 extremely rapidly within clonal bacterial populations, becoming a significant portion of the phage
206 population in 18 hours or approximately <7 population-wide bacterial generations. This rapid
207 miniphage invasion has also been reported for Pf4 infecting PAO1.[28] Eventually, through
208 subsequent uneven vertical inheritance of phages, we observed that some bacteria only inherit
209 Pf5*mini (Fig 1D). Once this happens, Pf5*mini can no longer leave the cell, and in following cell
210 divisions, the bacteria lose the phage completely (PA14ΔPf5; Fig 1E). This process defines a
211 Tragedy of the Commons for the Pf phages as competition leads to the complete loss of full-
212 length phage genomes that can produce capsid and thus the phage population goes locally
213 extinct. Nonetheless, WGS of PA14ΔPf5 shows that the *pf5* attachment sites in PA14ΔPf5
214 remain intact, indicating the possibility for reinfection. We competed PA14ΔPf5 directly against
215 PA14 WT and found it lost the competitive advantage of the original PA14* genotype, implying
216 that the phage-free state is ecologically unstable and prone to reinfection and re-initiation of this
217 life cycle (Supp. Figure 3).
218
219 **Discussion**
220
221 Molecular parasites such as phages can increase their evolutionary potential and fitness
222 by expanding their population size. In such conditions, multiple genotypes can arise and
223 cooccur within a host cell, including defective variants that can be rescued and persist through
224 complementation by complete phage genomes.[29,30] However, large parasite populations
225 increase the burden on the host, leading to greater conflict between host and parasite and also
226 greater intracellular conflict between parasites as competition for host resources ramp up. In
227 addition, genetic and phenotypic diversification of these molecular parasites can affect host
228 fitness and introduce diversity between infected cells. Many bacteria carry prophages in their
229 genomes, and *P. aeruginosa* and their widespread Pf prophage are no exception.[10] While some
230 aspects of bacteria and phage interaction can be mutualistic, such as the provision of antibiotic
231 resistance genes and superinfection exclusion mechanisms, this pact can quickly shift towards
232 parasitism. Here, we show that bacteria can be at the mercy of rapid changes in their prophage
233 population developing in mere hours that slow bacterial reproduction but transiently increase
234 relative bacterial fitness. Specifically, we report that Pf phages that evolved a defective Pf
235 repressor provide the bacterial host with the ability to use Pf as a weapon against other bacterial

236 competitors, but that this state is unstable: the emergence and spread of cheater miniphages
237 result in a phage Tragedy of the Commons and can lead to subsequent phage extinction.
238 Viruses can cheat other viruses infecting the same host by not contributing to public
239 goods production.[31] For example, viruses lacking capsid genes do not contribute to capsid
240 production but can use capsid proteins produced by co-infecting "cooperative" viruses, thereby
241 selfishly propagating at the expense of the cooperators. Filamentous phages, including M13 and
242 f1 that infect *E. coli* and Pf4 in PAO1, have been observed to lose large parts of their genome
243 creating cheater miniphages.[28,32–35] These miniphages have been reported in *P. aeruginosa* Pf
244 previously[28,36] and one study created miniphages by deleting structural genes[37], but otherwise,
245 Pf miniphages have not been actively studied. When phage replication is rampant, miniphages
246 arising initially at low frequency gain a large fitness advantage as they have many cooperators
247 to exploit. In Pf4 phages of *P. aeruginosa*, deletion of the Pf4 repressor (*pf4r*) gene was
248 observed to increase phage production[18] and to produce Pf superinfective variants that increase
249 intracellular phage diversity.[19,38] These superinfective Pf variants were reported to kill their host
250 cell and play roles in bacterial biofilm dispersal and in phenotypes such as small colony variants
251 and bacterial virulence.[17,21,22,38–40] In this study, we show that the emergence of superinfective
252 Pf5 variants in strain PA14 leads to the subsequent invasion of Pf miniphages and a rapid
253 sequence of events affecting bacterial fitness. We were able to detect these dynamics by
254 sequencing whole genomes of bacterial clones and populations over short intervals and
255 focusing on spikes in read depth as well as reads that support circularization of the Pf5
256 prophage genome. This study presents both a conceptual model and analytical methods for
257 interpreting the genomes of bacteria carrying filamentous phage, which may reveal ongoing
258 interactions in their intracellular virome.
259 In summary, we demonstrate that intracellular phage competition can favor rapid
260 expansion of the phage population both within and among neighboring host bacteria, but this
261 evolution is short-sighted, as short-term gains in phage fitness lead to their eventual local
262 extinction. From the perspective of the bacterial cell, its fitness is aligned with the hyper-
263 replicative phage at the outset, because the cost of phage replication is outweighed by
264 increased relative fitness against other cells becoming superinfected. The emergence of cheater
265 phages also benefits the host by improving immunity against further superinfection, but it dooms
266 the phage to a Tragedy of the Commons and extinction. Phage loss eliminates any burdens of
267 phage replication for the host but it also eliminates the relative fitness advantage of infected
268 cells, leaving the bacterial population susceptible to invasion.

269 Superinfective variants of Pf can readily appear and have been documented to be an
270 important part of *P. aeruginosa* lifestyle relevant for a broad array of clinically important bacterial
271 phenotypes, especially in biofilm.[14,19,21,36,41] This study shows that the emergence of such hyper
272 replicative and superinfective variants favors the invasion of miniphages both within and among
273 host cells. But since Pf phage population structure can shift in a manner of hours and affect
274 bacterial fitness, antimicrobial resistance, defense against host immunity, and aspects of
275 pathogenicity[10,11,13,15], our study reveals a potentially common yet overlooked driver of *P.*
276 *aeruginosa* evolution and potentially of all bacteria harboring filamentous phages.[42]
277
278
279 **Methods**
280
281 **Bacteria strains and culture conditions**
282 *Pseudomonas aeruginosa* UCBPP-PA14 *pf5r* mutant clones were originally isolated
283 from an evolution experiment, but these mutants contained secondary mutations.[16,20] To create
284 a *pf5r* mutant in the PA14 WT background (PA14*full), we co-cultured an unmarked, evolved
285 PA14 *pf5r* mutant with *lacZ*-marked PA14 WT overnight and screened blue colonies for
286 mobilized Pf5 *pf5r* phage via qPCR across the attachment sites (attB and attP) for excised and
287 circularized Pf phage, respectively, with *gyrB* as the housekeeping gene. Colonies with high
288 copy number for attB and attP were analyzed by whole genome sequencing (WGS) to confirm
289 presence of the *pf5r* mutation via horizontal gene transfer. PA14*full/mini and PA14*mini were
290 isolated by streaking PA14*full on 1/2 Tryptic Soy (Tsoy) Agar and screening colonies for capsid
291 deletion via PCR. PA14ΔPf5 was isolated by streaking PA14*mini on 1/2 Tsoy agar and
292 screening across two conserved phage genes in Pf5*mini (i.e., PA14_48980-PA14_489900). All
293 mutants were verified via WGS. PA14Δ*pilA* mutant was generated through two-step allelic
294 exchange[43] and confirmed via WGS. Bacteria were cultured in glass tubes at 37˚C on a roller
295 drum with M9 minimal media supplemented with nutrients found in cystic fibrosis lungs (i.e. CF
296 media) as previously described.[16] In short, the media comprised of an M9 salt base (0.1 mM
297 $CaCl_2$,1.0 mM $MgSO_4$, 42.2 mM Na_2HPO_4, 22 mM KH_2PO_4, 21.7 mM NaCl, 18.7 mM NH_4Cl),
298 11.1 mM glucose, 10 mM DL-lactate (Sigma-Aldrich 72-17-3), 20 mL/liter MEM essential amino
299 acids (ThermoFisher 11130051), 10 mL/liter MEM non-essential amino acids (ThermoFisher
300 11140050), and 1 mL/liter each of Trace Elements A, B, and C (Corning 99182CL, 99175CL,
301 99176CL).
302

303 **Whole genome sequencing and analysis**

304 DNA of all bacteria strains were extracted using the Qiagen DNeasy Blood & Tissue Kit
305 and WGS using Illumina NextSeq550 with a resolution of 200 Mbp or between 3-14 million
306 reads per sample. Reads were checked in fastQC[44] for quality control. The PA14 WT reads
307 were mapped against the PA14 from the Pseudomonas Genome Database[45,47]
308 (https://www.pseudomonas.com/strain/show/109) using the variant caller breseq v0.39.0[46] with
309 the consensus mode default parameters. Then the gdtools program within breseq was used to
310 create a new PA14 reference genome that contains mutations present in our PA14 lab wildtype
311 strain. Raw reads of all other samples were mapped against this new reference. Read depth
312 was calculated by averaging the reads mapped to a 10bp window across the bacterial genome
313 using bedtools[48] (v2.26.0) and samtools[49] (v1.21). The raw reads have been deposited with
314 links to BioProject accession number PRJNA692838 and PRJNA1226961 in the NCBI
315 BioProject database (https://www.ncbi.nlm.nih.gov/bioproject/). Read depth plots were created
316 using R[52] (v4.4.0), RStudio[53] (v2024.04.2+764), tidyverse[54] (v2.0.0), ggplot2[55] (v3.5.1), and
317 gggenes[56] (v0.5.1).
318
319

320 **Growth curves**

321 Growth curves were conducted in 96-well plates with each well seeded with 198µL of CF
322 media and 2µL overnight bacterial culture. Optical density was read at 600nm (OD_{600}) every 15
323 minutes over the course of 24 hours at 37°C. OD_{600} was graphed in R, and the growth rate, area
324 under the curve (AUC), and the final OD_{600} was calculated using the Growthcurver package.[50]
325

326 **Competition assays**

327 Overnight cultures of each competitor strain were grown in individual tubes in CF media
328 at 37°C prior to the competition. Competitors were paired such that one competitor was *lacZ*-
329 marked while the other was unmarked. Approximately 1mL of overnight cultures were pelleted
330 and washed with 1xPBS to remove phages that may be present in the supernatant. The paired
331 competitors were mixed at varying ratios so that the total volume of the co-culture was 50 µL
332 and this was seeded into 5 mL of fresh CF media to make a 1:100 dilution. For competitions
333 where CFU/mL were measured multiple times between timepoints 0h and 24h, a 1:1 volume
334 ratio was used to seed competitions where *pf5r* mutants were rare relative to their competitors
335 (either PA14 WT or PA14Δ*pilA*). For competitions where *pf5r* mutants were approximately 1:1 in
336 starting CFU/mL with competitors, a 1:9 volume ratio of competitor-to-*pf5r* culture was used.

337 The co-cultures were then vortexed and starting CFU/mL (t=0h) was quantified by serial diluting
338 the co-cultures in 1xPBS and spread plating the dilutions onto 1/2 Tryptic Soy Agar plates
339 supplemented with Xgal. The co-cultures were then incubated at 37°C on a roller drum and
340 CFU/mL was measured at various timepoints using plate dilutions up until 24h post-inoculation.
341 Blue and white colonies were counted, and selection rate constant (r) was calculated by taking
342 the difference in Malthusian parameter of the two competitors[51]: $r = \ln\left(\frac{M_f}{M_i}\right) - \ln\left(\frac{A_f}{A_i}\right)$, where M_i
343 and A_i is the mutant or ancestor CFU/mL at 0h post-inoculation, respectively, and M_f and A_f is
344 their CFU/mL at 24h post-inoculation, respectively.
345
346 **Pf5* phage treatment on PA14 WT and PA14Δ*pilA***
347 Overnight cultures of PA14 WT, PA14Δ*pilA*, PA14*full, and PA14*full/mini were grown in
348 CF media at 37°C. Approximately 1mL of PA14*full and PA14*full/mini overnight cultures were
349 passed through a 0.20μm filter into separate microcentrifuge tubes. Then into 5mL of fresh CF
350 media, 50μL of the filtrate and 50μL of the PA14 WT or PA14Δ*pilA* overnight were added and
351 vortexed. The CFU/mL of the initial culture (0h) was measured by taking 20μL of the seeded
352 culture and doing ten-fold dilutions in a 96-well plate with 1xPBS. 100μL of the diluted culture
353 was plated onto 1/2 Tsoy supplemented with Xgal before incubating the plates overnight. The
354 culture tubes were removed from the incubator at 2h, 4h, 6h, and 24h to measure CFU/mL as
355 described earlier.
356
357 **Twitching assay**
358 Twitching motility were measured following an established protocol.[24] Briefly, a single
359 colony from the competition experiments (either the 0h timepoint or 24h timepoints) were picked
360 using a pipette tip. The colony color was used to distinguish PA14*full and PA14*full/mini (blue;
361 *lacZ*-marked) from PA14 WT (white; unmarked). The center of the 1% LB-Lennox Agar was
362 stabbed using the pipette tip, making sure that the tip touched the bottom of the petri dish. Then,
363 the plates were incubated at 37°C overnight in a plastic container with a lid and lined with damp
364 paper towels to prevent the plates from drying. The following day, plates were flooded with cold
365 TM developer solution for 30 minutes to make the bacteria opaque. Twitching distance was
366 measured from the center of the plate where the stabs were made to the edge of the front using
367 a ruler.
368
369 **Data Availability**

All raw reads from the whole genome sequencing have been deposited with links to BioProject accession number PRJNA692838 and PRJNA1226961 in the NCBI BioProject database (https://www.ncbi.nlm.nih.gov/bioproject/). Data and scripts used to analyze variant calls, read depth, growth curves, competition assays, and twitch assays can be found at https://github.com/NanamiKubota/pf_cheater_phage.

Acknowledgments

We thank members of the Cooper lab, the Pat Secor lab, and thesis committee members (Drs. Daria Van Tyne, Will DePas, Graham Hatfull, and Pat Secor) for valuable feedback and support. Research was supported in part by the Ruth L. Kirschstein Predoctoral Individual National Research Service Award (1F31AI179118-01 to NK), by NIH U19AI158076 to VSC, and by the Pennsylvania Department of Health PA CURES Grant #4100085725. The content is solely the responsibility of the authors and does not necessarily represent the official views of the National Institutes of Health or the Pennsylvania Department of Health.

Author contributions

Conceptualization, writing, review, and final approval of the manuscript were done by NK, MRS, and VSC. Experiment and bioinformatics analyses were done by NK and MRS.

1. Schmidt, A.K., Schwartzkopf, C.M., Pourtois, J.D., Burgener, E.B., Faith, D.R., Joyce, A., Lamma, T., Kumar, G., Bollyky, P.L., and Secor, P.R. (2024). Targeted deletion of Pf prophages from diverse Pseudomonas aeruginosa isolates has differential impacts on quorum sensing and virulence traits. Journal of Bacteriology *0*, e00402-23. https://doi.org/10.1128/jb.00402-23.

2. Schwartzkopf, C.M., Robinson, A.J., Ellenbecker, M., Faith, D.R., Schmidt, A.K., Brooks, D.M., Lewerke, L., Voronina, E., Dandekar, A.A., and Secor, P.R. (2023). Tripartite interactions between filamentous Pf4 bacteriophage, Pseudomonas aeruginosa, and bacterivorous nematodes. PLOS Pathogens *19*, e1010925. https://doi.org/10.1371/journal.ppat.1010925.

3. Secor, P.R., Michaels, L.A., Smigiel, K.S., Rohani, M.G., Jennings, L.K., Hisert, K.B., Arrigoni, A., Braun, K.R., Birkland, T.P., Lai, Y., et al. (2016). Filamentous Bacteriophage Produced by Pseudomonas aeruginosa Alters the Inflammatory Response and Promotes Noninvasive Infection In Vivo. Infect Immun *85*, e00648-16. https://doi.org/10.1128/IAI.00648-16.

4. Thomas, M.J.N., Brockhurst, M.A., and Coyte, K.Z. (2024). What makes a temperate phage an effective bacterial weapon? mSystems *0*, e01036-23. https://doi.org/10.1128/msystems.01036-23.

5. Wang, X., Kim, Y., Ma, Q., Hong, S.H., Pokusaeva, K., Sturino, J.M., and Wood, T.K. (2010). Cryptic prophages help bacteria cope with adverse environments. Nat Commun *1*, 147. https://doi.org/10.1038/ncomms1146.

6. Wendling, C.C., Refardt, D., and Hall, A.R. (2021). Fitness benefits to bacteria of carrying prophages and prophage-encoded antibiotic-resistance genes peak in different environments. Evolution *75*, 515–528. https://doi.org/10.1111/evo.14153.

7. Schmidt, A.K., Fitzpatrick, A.D., Schwartzkopf, C.M., Faith, D.R., Jennings, L.K., Coluccio, A., Hunt, D.J., Michaels, L.A., Hargil, A., Chen, Q., et al. (2022). A Filamentous Bacteriophage Protein Inhibits Type IV Pili To Prevent Superinfection of Pseudomonas aeruginosa. mBio *13*. https://doi.org/10.1128/mbio.02441-21.

8. Marvin, D.A., and Hohn, B. (1969). Filamentous Bacterial Viruses. Bacteriological reviews *33*, 172–209.

9. Bradley, D.E. (1974). The adsorption of Pseudomonas aeruginosa pilus-dependent bacteriophages to a host mutant with nonretractile pili. Virology *58*, 149–163. https://doi.org/10.1016/0042-6822(74)90150-0.

10. Burgener, E.B., Sweere, J.M., Bach, M.S., Secor, P.R., Haddock, N., Jennings, L.K., Marvig, R.L., Johansen, H.K., Rossi, E., Cao, X., et al. (2019). Filamentous bacteriophages are associated with chronic Pseudomonas lung infections and antibiotic resistance in cystic fibrosis. Science Translational Medicine *11*, eaau9748. https://doi.org/10.1126/scitranslmed.aau9748.

11. Secor, P.R., Burgener, E.B., Kinnersley, M., Jennings, L.K., Roman-Cruz, V., Popescu, M., Van Belleghem, J.D., Haddock, N., Copeland, C., Michaels, L.A., et al. (2020). Pf Bacteriophage and Their Impact on Pseudomonas Virulence, Mammalian Immunity, and

430 Chronic Infections. Frontiers in Immunology *11*, 1–18.
431 https://doi.org/10.3389/fimmu.2020.00244.

432 12. Cystic Fibrosis Foundation Patient Registry 2022 Annual Data Report Bethesda, Maryland
433 ©2023 Cystic Fibrosis Foundation

434 13. Chen, Q., Cai, P., Chang, T.H.W., Burgener, E., Kratochvil, M.J., Gupta, A., Hargill, A.,
435 Secor, P.R., Nielsen, J.E., Barron, A.E., et al. (2024). Pf bacteriophages hinder sputum
436 antibiotic diffusion via electrostatic binding. Science Advances *10*, eadl5576.
437 https://doi.org/10.1126/sciadv.adl5576.

438 14. Secor, P.R., Sweere, J.M., Michaels, L.A., Malkovskiy, A.V., Lazzareschi, D., Katznelson,
439 E., Rajadas, J., Birnbaum, M.E., Arrigoni, A., Braun, K.R., et al. (2015). Filamentous
440 bacteriophage promote biofilm assembly and function. Cell Host and Microbe *18*, 549–559.
441 https://doi.org/10.1016/j.chom.2015.10.013.

442 15. Bach, M.S., de Vries, C.R., Khosravi, A., Sweere, J.M., Popescu, M.C., Chen, Q.,
443 Demirdjian, S., Hargil, A., Van Belleghem, J.D., Kaber, G., et al. (2022). Filamentous
444 bacteriophage delays healing of Pseudomonas-infected wounds. Cell Reports Medicine *3*,
445 100656. https://doi.org/10.1016/j.xcrm.2022.100656.

446 16. Scribner, M.R., Stephens, A.C., Huong, J.L., Richardson, A.R., and Cooper, V.S. (2022).
447 The nutritional environment is sufficient to select coexisting biofilm and quorum-sensing
448 mutants of Pseudomonas aeruginosa. Journal of Bacteriology, JB-00444.
449 https://doi.org/10.1128/JB.00444-21.

450 17. Ismail, M.H., Michie, K.A., Goh, Y.F., Noorian, P., Kjelleberg, S., Duggin, I.G., McDougald,
451 D., and Rice, S.A. (2021). The Repressor C Protein, Pf4r, Controls Superinfection of
452 Pseudomonas aeruginosa PAO1 by the Pf4 Filamentous Phage and Regulates Host Gene
453 Expression. Viruses *13*, 1614. https://doi.org/10.3390/v13081614.

454 18. Li, Y., Liu, X., Tang, K., Wang, P., Zeng, Z., Guo, Y., and Wang, X. (2019). Excisionase in
455 Pf filamentous prophage controls lysis-lysogeny decision-making in Pseudomonas
456 aeruginosa. Molecular Microbiology *111*, 495–513. https://doi.org/10.1111/mmi.14170.

457 19. McElroy, K.E., Hui, J.G.K., Woo, J.K.K., Luk, A.W.S., Webb, J.S., Kjelleberg, S., Rice, S.A.,
458 and Thomas, T. (2014). Strain-specific parallel evolution drives short-term diversification
459 during Pseudomonas aeruginosa biofilm formation. Proceedings of the National Academy of
460 Sciences of the United States of America *111*. https://doi.org/10.1073/pnas.1314340111.

461 20. Scribner, M.R., Santos-Lopez, A., Marshall, C.W., Deitrick, C., and Cooper, V.S. (2020).
462 Parallel Evolution of Tobramycin Resistance across Species and Environments. mBio *11*,
463 1–17. https://doi.org/10.1128/mBio.00932-20.

464 21. Rice, S.A., Tan, C.H., Mikkelsen, P.J., Kung, V., Woo, J., Tay, M., Hauser, A., McDougald,
465 D., Webb, J.S., and Kjelleberg, S. (2009). The biofilm life cycle and virulence of
466 Pseudomonas aeruginosa are dependent on a filamentous prophage. ISME J *3*, 271–282.
467 https://doi.org/10.1038/ismej.2008.109.

468 22. Tortuel, D., Tahrioui, A., Rodrigues, S., Cambronel, M., Boukerb, A.M., Maillot, O., Verdon,
469 J., Bere, E., Nusser, M., Brenner-Weiss, G., et al. (2020). Activation of the Cell Wall Stress

470 Response in Pseudomonas aeruginosa Infected by a Pf4 Phage Variant. Microorganisms *8*,
471 1700. https://doi.org/10.3390/microorganisms8111700.

472 23. Burrows, L.L. (2012). Pseudomonas aeruginosa Twitching Motility: Type IV Pili in Action.
473 Annu. Rev. Microbiol. *66*, 493–520. https://doi.org/10.1146/annurev-micro-092611-150055.

474 24. Turnbull, L., and Whitchurch, C.B. (2014). Motility Assay: Twitching Motility. In
475 Pseudomonas Methods and Protocols, A. Filloux and J.-L. Ramos, eds. (Springer), pp. 73–
476 86. https://doi.org/10.1007/978-1-4939-0473-0_9.

477 25. Wang, W., Li, Y., Tang, K., Lin, J., Gao, X., Guo, Y., and Wang, X. (2022). Filamentous
478 prophage capsid proteins contribute to superinfection exclusion and phage defence in
479 Pseudomonas aeruginosa. Environmental Microbiology *24*, 4285–4298.
480 https://doi.org/10.1111/1462-2920.15991.

481 26. Chung, I.-Y., Jang, H.-J., Bae, H.-W., and Cho, Y.-H. (2014). A phage protein that inhibits
482 the bacterial ATPase required for type IV pilus assembly. Proceedings of the National
483 Academy of Sciences *111*, 11503–11508. https://doi.org/10.1073/pnas.1403537111.

484 27. Bondy-Denomy, J., Qian, J., Westra, E.R., Buckling, A., Guttman, D.S., Davidson, A.R., and
485 Maxwell, K.L. (2016). Prophages mediate defense against phage infection through diverse
486 mechanisms. ISME Journal *10*, 2854–2866. https://doi.org/10.1038/ismej.2016.79.

487 28. Secor, P.R., and Dandekar, A.A. (2020). More than simple parasites: The sociobiology of
488 bacteriophages and their bacterial hosts. mBio *11*. https://doi.org/10.1128/mBio.00041-20.

489 29. Nee, S., and Smith, J.M. (1990). The evolutionary biology of molecular parasites.
490 Parasitology *100*, S5–S18. https://doi.org/10.1017/S0031182000072978.

491 30. Stern, A., and Andino, R. (2016). Chapter 17 - Viral Evolution: It Is All About Mutations. In
492 Viral Pathogenesis (Third Edition), M. G. Katze, M. J. Korth, G. L. Law, and N. Nathanson,
493 eds. (Academic Press), pp. 233–240. https://doi.org/10.1016/B978-0-12-800964-2.00017-3.

494 31. Leeks, A., West, S.A., and Ghoul, M. (2021). The evolution of cheating in viruses. Nature
495 Communications *12*, 6928. https://doi.org/10.1038/s41467-021-27293-6.

496 32. Griffith, J., and Kornberg, A. (1974). Mini M13 bacteriophage: Circular fragments of M13
497 DNA are replicated and packaged during normal infections. Virology *59*, 139–152.
498 https://doi.org/10.1016/0042-6822(74)90211-6.

499 33. Enea, V., and Zinder, N.D. (1975). A deletion mutant of bacteriophage f1 containing no
500 intact cistrons. Virology *68*, 105–114. https://doi.org/10.1016/0042-6822(75)90152-X.

501 34. Hewitt, J.A. (1975). Miniphage − a Class of Satellite Phage to M13. Journal of General
502 Virology *26*, 87–94. https://doi.org/10.1099/0022-1317-26-1-87.

503 35. Horiuchi, K. (1983). Co-evolution of a filamentous bacteriophage and its defective interfering
504 particles. Journal of Molecular Biology *169*, 389–407. https://doi.org/10.1016/S0022-
505 2836(83)80057-6.

506 36. Guo, Y., Lin, S., Chen, R., Gu, J., Tang, K., Nie, Z., Huang, Z., Weng, J., Lin, J., Liu, T., et
507 al. (2024). A reverse transcriptase controls prophage genome reduction to promote phage
508 dissemination in *Pseudomonas aeruginosa* biofilms. Cell Reports *43*, 114883.
509 https://doi.org/10.1016/j.celrep.2024.114883.

510 37. Pei, T.-T., Luo, H., Wang, Y., Li, H., Wang, X.-Y., Zhang, Y.-Q., An, Y., Wu, L.-L., Ma, J.,
511 Liang, X., et al. (2024). Filamentous prophage Pf4 promotes genetic exchange in
512 Pseudomonas aeruginosa. The ISME Journal *18*, wrad025.
513 https://doi.org/10.1093/ismejo/wrad025.

514 38. Prokopczuk, F.I., Im, H., Campos-Gomez, J., Orihuela, C.J., and Martínez, E. (2023).
515 Engineered Superinfective Pf Phage Prevents Dissemination of Pseudomonas aeruginosa
516 in a Mouse Burn Model. mBio *0*, e00472-23. https://doi.org/10.1128/mbio.00472-23.

517 39. Hui, J.G.K., Mai-Prochnow, A., Kjelleberg, S., McDougald, D., and Rice, S.A. (2014).
518 Environmental cues and genes involved in establishment of the superinfective Pf4 phage of
519 Pseudomonas aeruginosa. Frontiers in Microbiology *5*, 1–8.
520 https://doi.org/10.3389/fmicb.2014.00654.

521 40. Tortuel, D., Tahrioui, A., David, A., Cambronel, M., Nilly, F., Clamens, T., Maillot, O.,
522 Barreau, M., Feuilloley, M.G.J., Lesouhaitier, O., et al. (2022). Pf4 Phage Variant Infection
523 Reduces Virulence-Associated Traits in Pseudomonas aeruginosa. Microbiol Spectr,
524 e01548-22. https://doi.org/10.1128/spectrum.01548-22.

525 41. Gavric, D., and Knezevic, P. (2022). Filamentous Pseudomonas Phage Pf4 in the Context
526 of Therapy-Inducibility, Infectivity, Lysogenic Conversion, and Potential Application. Viruses
527 *14*, 1261. https://doi.org/10.3390/v14061261.

528 42. Foxall, R.L., Means, J., Marcinkiewicz, A.L., Schillaci, C., DeRosia-Banick, K., Xu, F., Hall,
529 J.A., Jones, S.H., Cooper, V.S., and Whistler, C.A. (2023). Inoviridae prophage and
530 bacterial host dynamics during diversification, succession, and Atlantic invasion of Pacific-
531 native Vibrio parahaemolyticus. mBio *15*, e02851-23. https://doi.org/10.1128/mbio.02851-
532 23.

533 43. Hmelo, L.R., Borlee, B.R., Almblad, H., Love, M.E., Randall, T.E., Tseng, B.S., Lin, C., Irie,
534 Y., Storek, K.M., Yang, J.J., et al. (2015). Precision-engineering the Pseudomonas
535 aeruginosa genome with two-step allelic exchange. Nat Protoc *10*, 1820–1841.
536 https://doi.org/10.1038/nprot.2015.115.

537 44. Andrews, S. (2010). FastQC: A Quality Control Tool for High Throughput Sequence Data.
538 http://www.bioinformatics.babraham.ac.uk/projects/fastqc/.

539 45. Winsor, G.L., Griffiths, E.J., Lo, R., Dhillon, B.K., Shay, J.A., and Brinkman, F.S.L. (2016).
540 Enhanced annotations and features for comparing thousands of Pseudomonas genomes in
541 the Pseudomonas genome database. Nucleic Acids Research *44*, D646–D653.
542 https://doi.org/10.1093/nar/gkv1227.

543 46. Deatherage, D.E., and Barrick, J.E. (2014). Identification of Mutations in Laboratory-Evolved
544 Microbes from Next-Generation Sequencing Data Using breseq. In, pp. 165–188.
545 https://doi.org/10.1007/978-1-4939-0554-6_12.

47. Lee, D.G., Urbach, J.M., Wu, G., Liberati, N.T., Feinbaum, R.L., Miyata, S., Diggins, L.T., He, J., Saucier, M., Déziel, E., et al. (2006). Genomic analysis reveals that Pseudomonas aeruginosa virulence is combinatorial. Genome Biol *7*, R90. https://doi.org/10.1186/gb-2006-7-10-r90.

48. Quinlan, A.R., and Hall, I.M. (2010). BEDTools: a flexible suite of utilities for comparing genomic features. Bioinformatics *26*, 841–842. https://doi.org/10.1093/bioinformatics/btq033.

49. Li, H., Handsaker, B., Wysoker, A., Fennell, T., Ruan, J., Homer, N., Marth, G., Abecasis, G., Durbin, R., and 1000 Genome Project Data Processing Subgroup (2009). The Sequence Alignment/Map format and SAMtools. Bioinformatics *25*, 2078–2079. https://doi.org/10.1093/bioinformatics/btp352.

50. Sprouffske, K., and Wagner, A. (2016). Growthcurver: an R package for obtaining interpretable metrics from microbial growth curves. BMC Bioinformatics *17*, 172. https://doi.org/10.1186/s12859-016-1016-7.

51. Travisano, M., and Lenski, R.E. (1996). Long-Term Experimental Evolution in Escherichia coli. IV. Targets of Selection and the Specificity of Adaptation. Genetics *143*, 15–26. https://doi.org/10.1093/genetics/143.1.15.

52. R Core Team (2024). R: a language and environment for statistical computing (R Foundation for Statistical Computing).

53. Posit team (2024). RStudio: Integrated development environment for R (Posit Software, PBC).

54. Wickham, H., Averick, M., Bryan, J., Chang, W., McGowan, L.D., François, R., Grolemund, G., Hayes, A., Henry, L., Hester, J., et al. (2019). Welcome to the tidyverse. Journal of Open Source Software *4*, 1686. https://doi.org/10.21105/joss.01686.

55. Wickham, H. (2016). ggplot2: Elegant graphics for data analysis (Springer-Verlag New York).

56. Wilkins, D. (2023). gggenes: Draw gene arrow maps in “ggplot2.”

575 **Figure legends**

576

577 **Figure 1. Emergence of hyper-replicative Pf5 phage (Pf5*full) leads to increased**
578 **intracellular phage diversity and eventual genome erosion.** The y-axis denotes the read
579 depth of the Pf5 prophage region relative to the average bacterial chromosome read depth
580 1000bp upstream and downstream of the prophage region. The yellow star on the gene map
581 denotes the position of the *pf5r* mutation. The red horizontal bars on the gene map denote the
582 attachment sites of the Pf5 phage. Read depths of (A) PA14 WT, (B) PA14*full, (C)
583 PA14*full/mini, (D) PA14*mini, and (E) PA14ΔPf5 are shown. PA14*mini (in D) shows that some
584 cells have already begun to lose Pf5 prophage completely as the read depth across the Pf5
585 prophage is lower than the read depth of the bacterial chromosome. (Created with
586 BioRender.com.)

587

588 **Figure 2. The *pf5r* mutation slows bacterial growth in monoculture but PA14*full/mini**
589 **rapidly invades and outcompetes PA14 WT by suppressing WT growth.** (A) Growth curve
590 of all genotypes over 24 hours (OD_{600}); (B) Final OD_{600} and area under the curve (AUC) of the
591 growth curves; (C) Top row: direct competitions begun with *pf5r* mutants rare and PA14 WT
592 common; bottom row: direct competitions begun with *pf5r* mutants and PA14 WT at 1:1 ratio,
593 with outcomes measured as CFU/ml of each competitor over time.

594

595 **Figure 3. Pf5*full and Pf5*mini phages suppress PA14 WT growth.** (A) Filtered supernatant
596 from overnight cultures of PA14 WT, PA14Δ*pilA*, PA14*full, PA14*full/mini, or no supernatant
597 was added to PA14 WT (left) or PA14Δ*pilA* (right) cultures. PA14*full/mini supernatant
598 (containing both Pf5*full and Pf5*mini phages) suppresses PA14 WT growth but not PA14Δ*pilA*,
599 which lacks the type 4 pili (T4P) phage receptor. (B) During competition against PA14 WT, both
600 PA14*full and PA14*full/mini exhibit reduced twitching motility mediated by TFP, with the latter
601 mutant to a greater extent.

602

603 **Figure 4. PA14*full and PA14*full/mini outcompete WT due to its greater susceptibility to**
604 **superinfection.** (A) Cell density (CFU/mL) of each competitor over time, in mixtures when *pf5r*
605 mutants are rare (top row) relative to PA14 WT, and in mixtures where *pf5r* mutants and PA14
606 WT begin at 1:1 ratio (bottom row). (B) Fitness of bacteria containing mutant phage (with
607 neutrality = 0) versus PA14 (top row) or PA14Δ*pilA* (bottom row) during competitions begun at a
608 range of frequencies (x-axis). PA14*full and especially PA14*full/mini outcompete WT at all

609 frequencies but are outcompeted by PA14Δ*pilA* due to its immunity to Pf5 superinfection. The
610 loss of Pf5 (PA14ΔPf5) also eliminates any competitive advantage against PA14 WT.
611
612 **Supplemental figure 1. Read depths of the phage genome normalized to the bacterial**
613 **chromosome show that read depth is higher across the prophage region in the**
614 **population from the evolution experiment where the Pf5 pf5r mutant phage was isolated**
615 **from.** Read depth was measured in 10 bp increments, and then they were normalized before
616 calculating for the mean and standard deviation for each Pf5 region.
617
618 **Supplemental figure 2. Read depths of the phage genome normalized to the bacterial**
619 **chromosome show that the phage copy number increases when *pf5r* is mutated and**
620 **increases again when both Pf5*full and Pf5*mini are present.** Read depth was measured in
621 10 bp increments, and then they were normalized before calculating for the mean and standard
622 deviation for each Pf5 region.
623
624 **Supplemental figure 3. Miniphage emergence occurs independently multiple times**
625 **following *pf5r* mutation.** Five bacterial clones carrying miniphage(s) were isolated, and the
626 horizontal lines denote the deletion edges of each clone's miniphage population. Some clones
627 (i.e. PA14*full/mini 3&4) carry multiple miniphage genotypes while others only have one (i.e.
628 PA14*full/mini 1&2 and PA14*mini). Deletion edges vary in their exact position but are
629 consistently in the same region, with all indicating loss of structural genes like capsid.
630
631 **Supplemental figure 4. CFU/mL measurements of the bacteria correlate with the OD_{600}**
632 **readings from Figure 2.** (A) Time course of CFU/mL for each strain and (B) CFU/mL
633 comparison at 24 hours.
634
635
636

Table 1.

Organism	Strain	Description	Accession	Origin
Bacteria	PA14 WT	*Pseudomonas aeruginosa* UCBPP-PA14 (also known as PA14) wildtype strain with wildtype Pf5 prophage and an intact *pf5r* gene.		(16)
	PA14*full	PA14 wildtype infected with full-length Pf5 phage with defective *pf5r* gene (i.e. Pf5*full phage).	SAMN23928097	(16)
	PA14*full/mini	PA14 infected by both Pf5*full and Pf5*mini phage.	SAMN46967948	This study
	PA14*mini	PA14 only infected by defective *pf5r* miniphage (Pf5*mini).	SAMN46967946	This study
	PA14ΔPf5	PA14 that lacks Pf5 phages/prophages but with an intact attB site.	SAMN46967947	This study
Phage	Pf5 WT	Wildtype Pf5 phage, usually found integrated into PA14 WT chromosome as a prophage and rarely induced.		(16)
	Pf5*full	Full-length Pf5 phage with defective *pf5r* gene isolated from the final evolved population of planktonic no drug cultures grown in CF media from a previous evolution experiment.		(16)
	Pf5*mini	Pf5 miniphage with defective *pf5r* gene that lost several genes, including the Pf5 capsid genes.		This study

Figure 1.

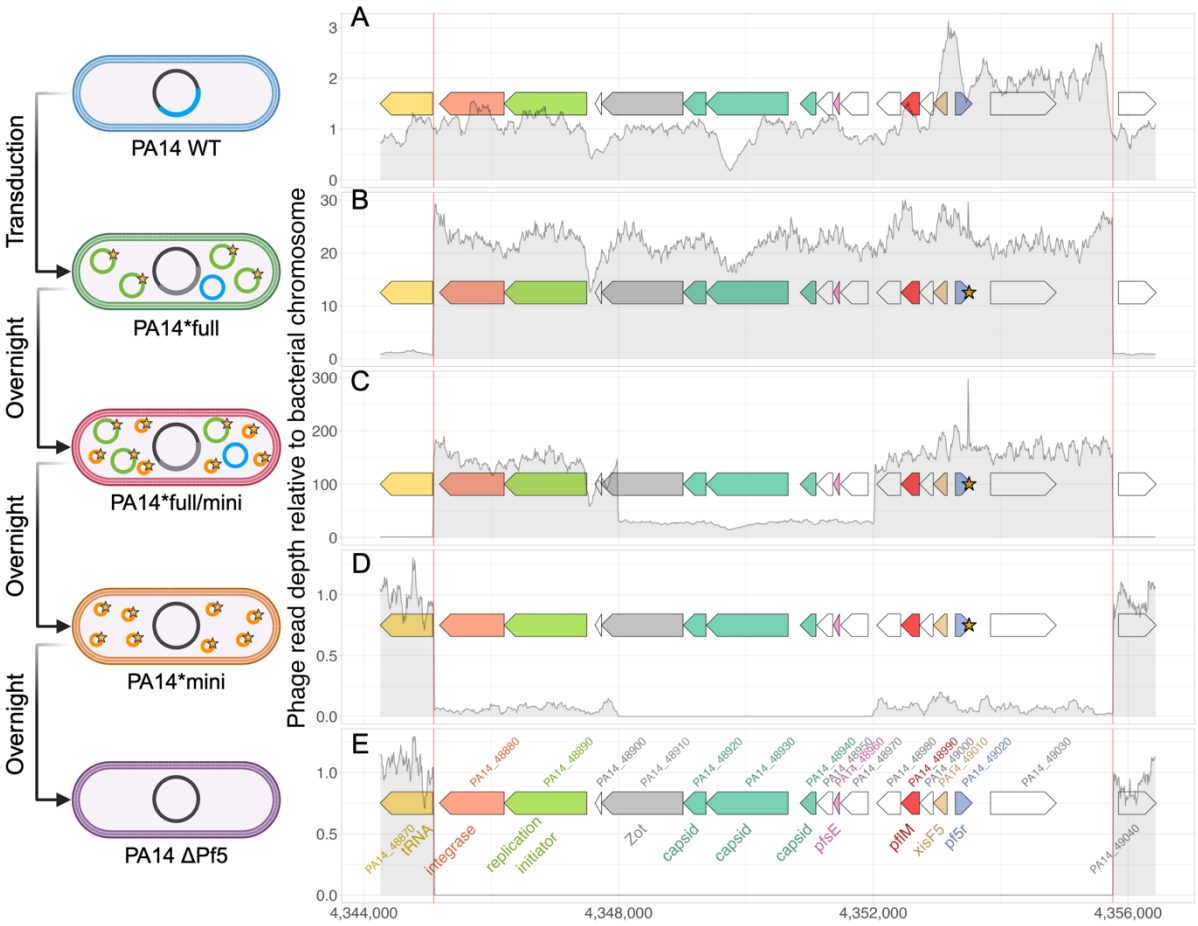
Transduction
Overnight
Overnight
Overnight
PA14 WT
PA14*full
PA14*full/mini
PA14*mini
PA14 ΔPf5
Phage read depth relative to bacterial chromosome
A
B
C
D
E
tRNA
integrase
replication initiator
Zot
capsid
capsid
capsid
pfsE
pflM
xisF5
pf5r
4,344,000
4,348,000
4,352,000
4,356,000

Figure 2.

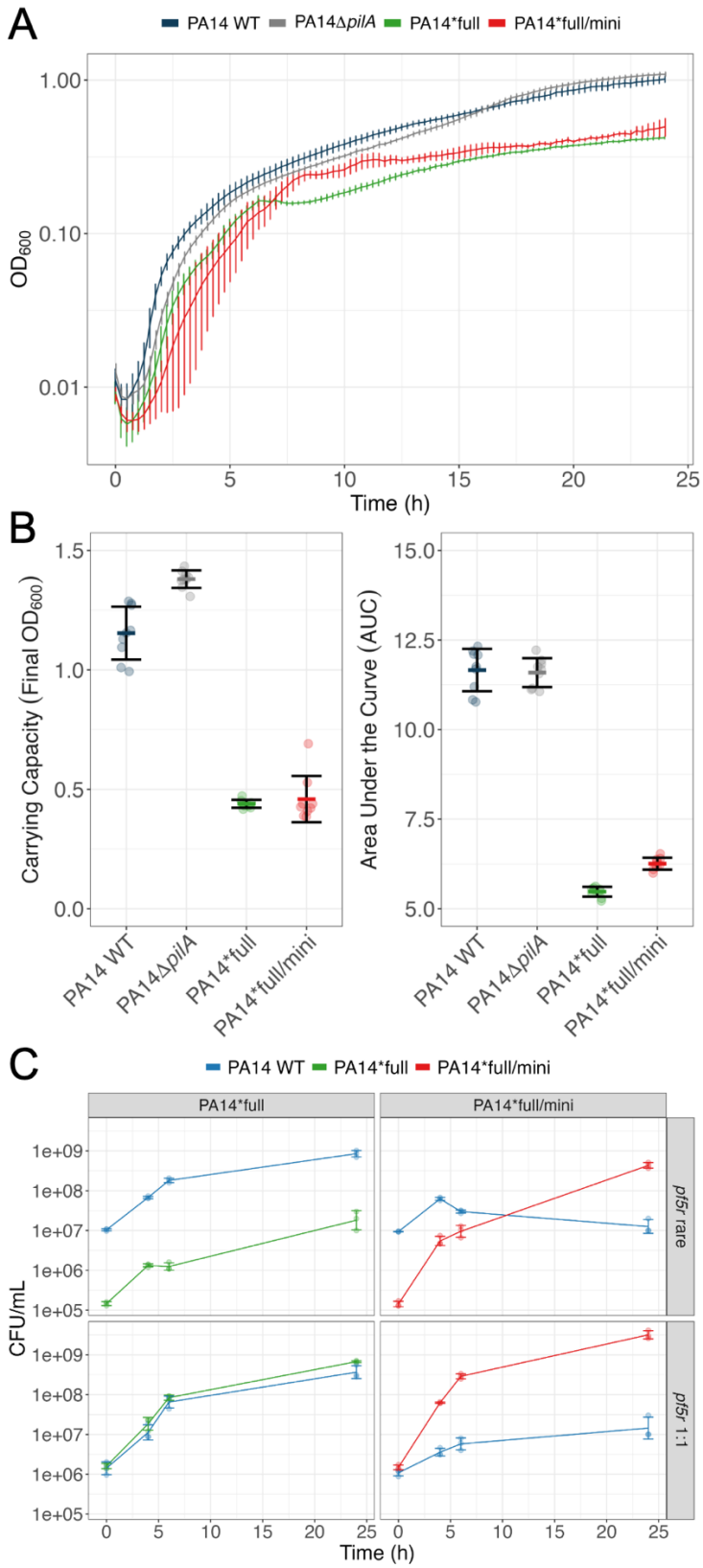
A
PA14 WT
PA14ΔpilA
PA14*full
PA14*full/mini
OD600
1.00
0.10
0.01
0
5
10
15
20
25
Time (h)
B
Carrying Capacity (Final OD600)
1.5
1.0
0.5
0.0
Area Under the Curve (AUC)
15.0
12.5
10.0
7.5
5.0
PA14 WT
PA14ΔpilA
PA14*full
PA14*full/mini
C
PA14 WT
PA14*full
PA14*full/mini
PA14*full
PA14*full/mini
pf5r rare
pf5r 1:1
CFU/mL
1e+09
1e+08
1e+07
1e+06
1e+05
0
5
10
15
20
25
Time (h)

Figure 3.

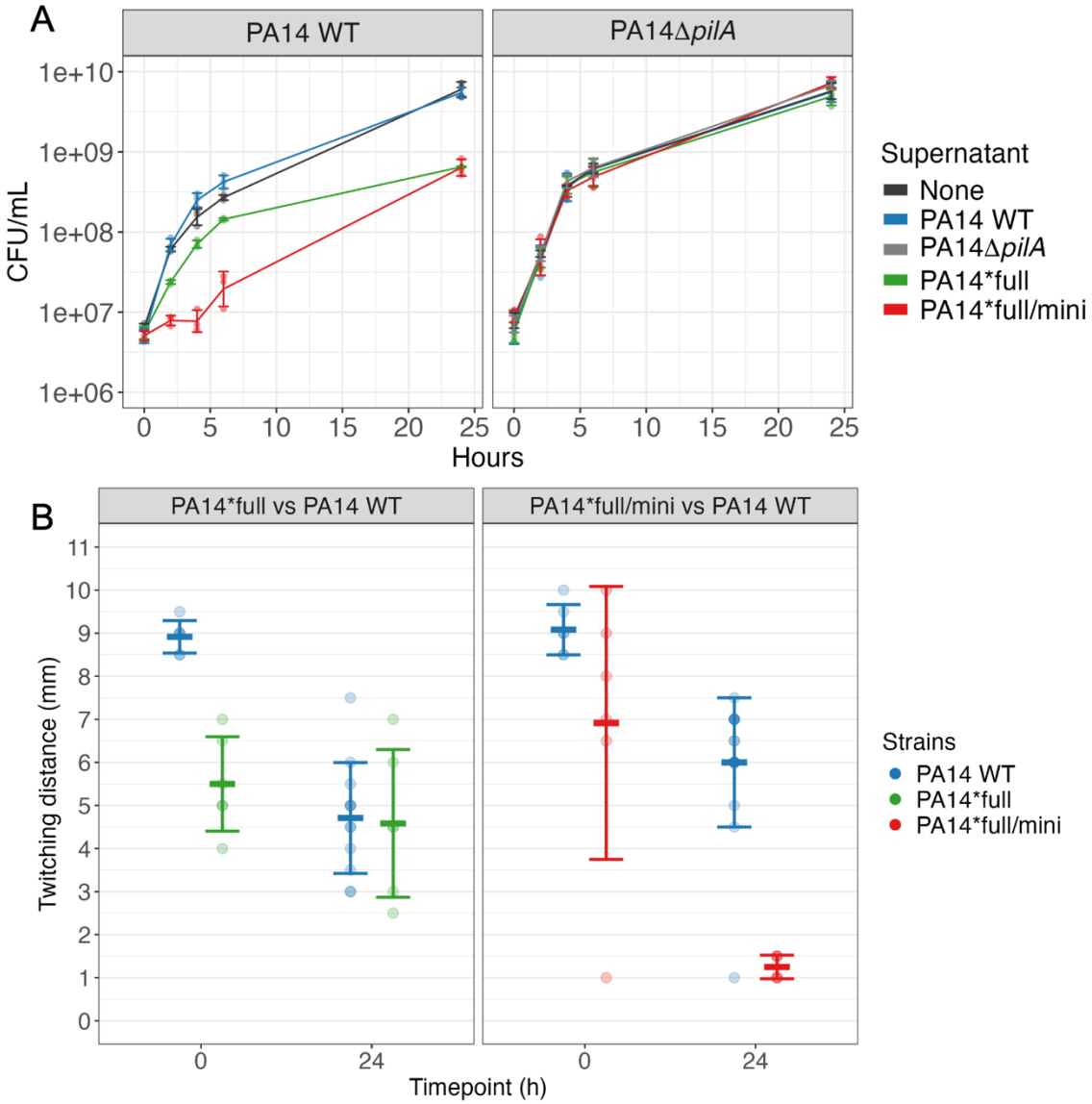
A
PA14 WT
PA14ΔpilA
CFU/mL
1e+10
1e+09
1e+08
1e+07
1e+06
0
5
10
15
20
25
Hours
Supernatant
None
PA14 WT
PA14ΔpilA
PA14*full
PA14*full/mini
B
PA14*full vs PA14 WT
PA14*full/mini vs PA14 WT
Twitching distance (mm)
11
10
9
8
7
6
5
4
3
2
1
0
24
Timepoint (h)
Strains
PA14 WT
PA14*full
PA14*full/mini

Figure 4.

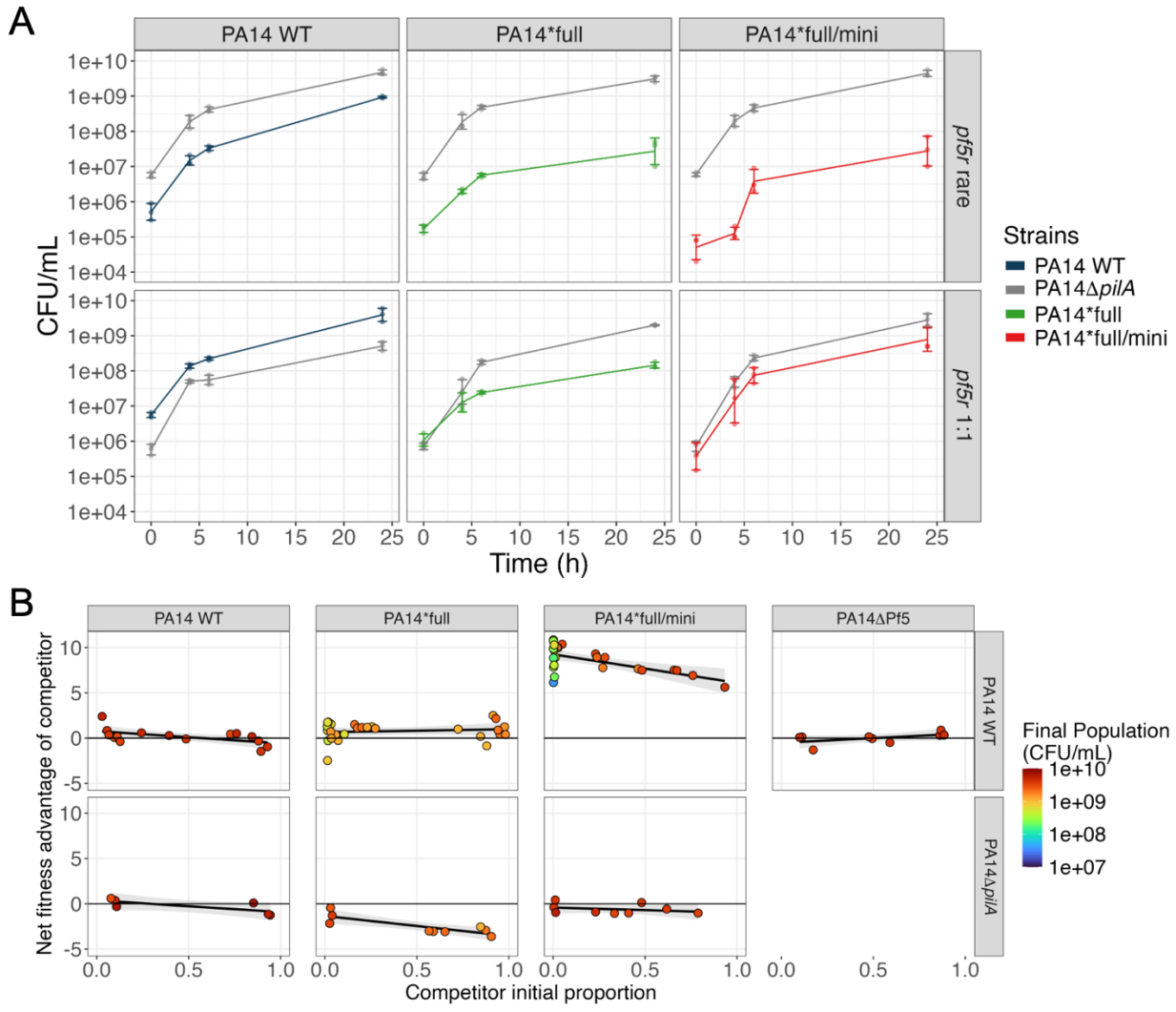
A
PA14 WT
PA14*full
PA14*full/mini
pf5r rare
pf5r 1:1
CFU/mL
1e+10
1e+09
1e+08
1e+07
1e+06
1e+05
1e+04
0
5
10
15
20
25
Time (h)
Strains
PA14 WT
PA14ΔpilA
PA14*full
PA14*full/mini
B
PA14 WT
PA14*full
PA14*full/mini
PA14ΔPf5
PA14ΔpilA
Net fitness advantage of competitor
10
5
0
-5
0.0
0.5
1.0
Competitor initial proportion
Final Population
(CFU/mL)
1e+10
1e+09
1e+08
1e+07

Supplemental Figures and Tables

Bacterial strain	mutated *pf5r*	Pf5 excision	Pf5 circularization
PA14 WT	0%	0%	2.7%
PA14*full	38.1%	16.7%	97.2%
PA14*full/mini	80.6%	5.8%	99.7%
PA14*mini	94.1%	97.1%	0%
PA14ΔPf5	0%	100%	0%

Supplemental table 1. Frequency of reads supporting *pf5r* mutation shows that clonal bacteria carry both mutated and wildtype copy of the *pf5r* gene until Pf5*mini phages drives phage population to a Tragedy of the Commons.

Name	Sequence (5'-3')	Purpose	Reference
PA14*gyrB*-f	cacagcatccagcgatacaag	qPCR housekeeping gene	(18)
PA14*gyrB*-r	cgcgttgctttcgatgaagt	qPCR housekeeping gene	(18)
Pf5-Cf	ttatgaccaacaccccaaacg	qPCR Pf5 circularization	(18)
Pf5-Cr	catttgtcgccggagtacct	qPCR Pf5 circularization	(18)
pf5 capsid F 1	cgcacgcttttcaatcctca	PCR Pf5 capsid gene	This study
pf5 capsid R 1	ctatctctcgctgttcgcgg	PCR Pf5 capsid gene	This study
pf5 capsid del F 1	attcggaatcggggacgatg	PCR Pf5 capsid gene loss	This study
pf5 capsid del R 1	gacgacgttgcgatagggat	PCR Pf5 capsid gene loss	This study
Pf miniphage F 1	ggtaacgatccctatcgcaa	PCR Pf5 miniphage	This study
Pf miniphage R 1	aagtactggcacgttgtgta	PCR Pf5 miniphage	This study
PA14-pilA-Up-R	aatatgcctgccctgactgc	*pilA* deletion cloning	This study
PA14-pilA-Up-F	gccagtgccaagcttgcatgcctgca ggtcgactctagaggcctcgcctgat agacaaca	*pilA* deletion cloning	This study
PA14-pilA-Down-R	agctatgaccatgattacgaattcgag ctcggtacccgggtcgccacaacgg aactactc	*pilA* deletion cloning	This study
PA14-pilA-Down-F	gcagtcagggcaggcatattgcatctt gcatgccaacctg	*pilA* deletion cloning	This study
M13 fwd	gtaaaacgacggccagt	*pilA* deletion cloning	universal primer
M13 rev	caggaaacagctatgac	*pilA* deletion cloning	universal primer
PA14-pilA-del-seq-F	ggccagcctgcagataagac	*pilA* deletion cloning	This study
PA14-pilA-del-seq-R	tcgatgatgatgccgagctt	*pilA* deletion cloning	This study

Supplemental Table 2. List of primers used in this study.

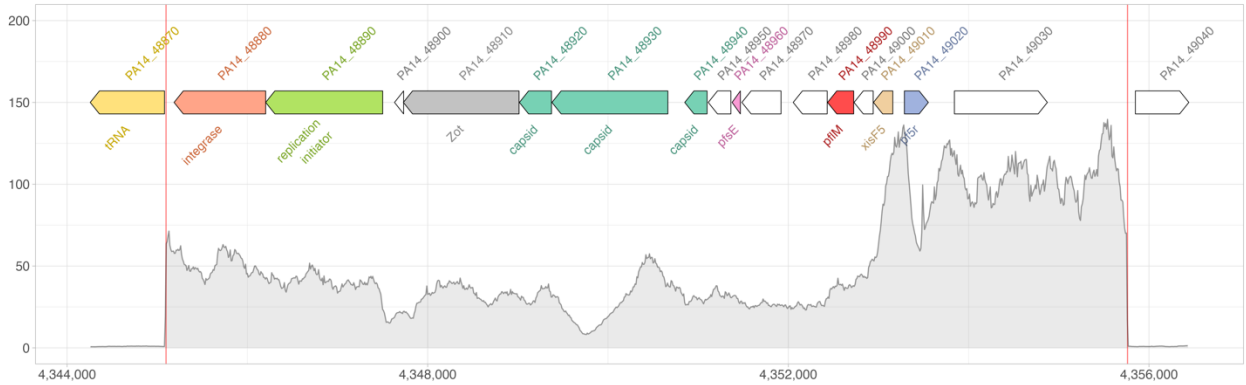

Supplemental figure 1. Read depths of the phage genome normalized to the bacterial chromosome show that read depth is higher across the prophage region in the population from the evolution experiment where the Pf5 pf5r mutant phage was isolated from. Read depth was measured in 10 bp increments, and then they were normalized before calculating for the mean and standard deviation for each Pf5 region.

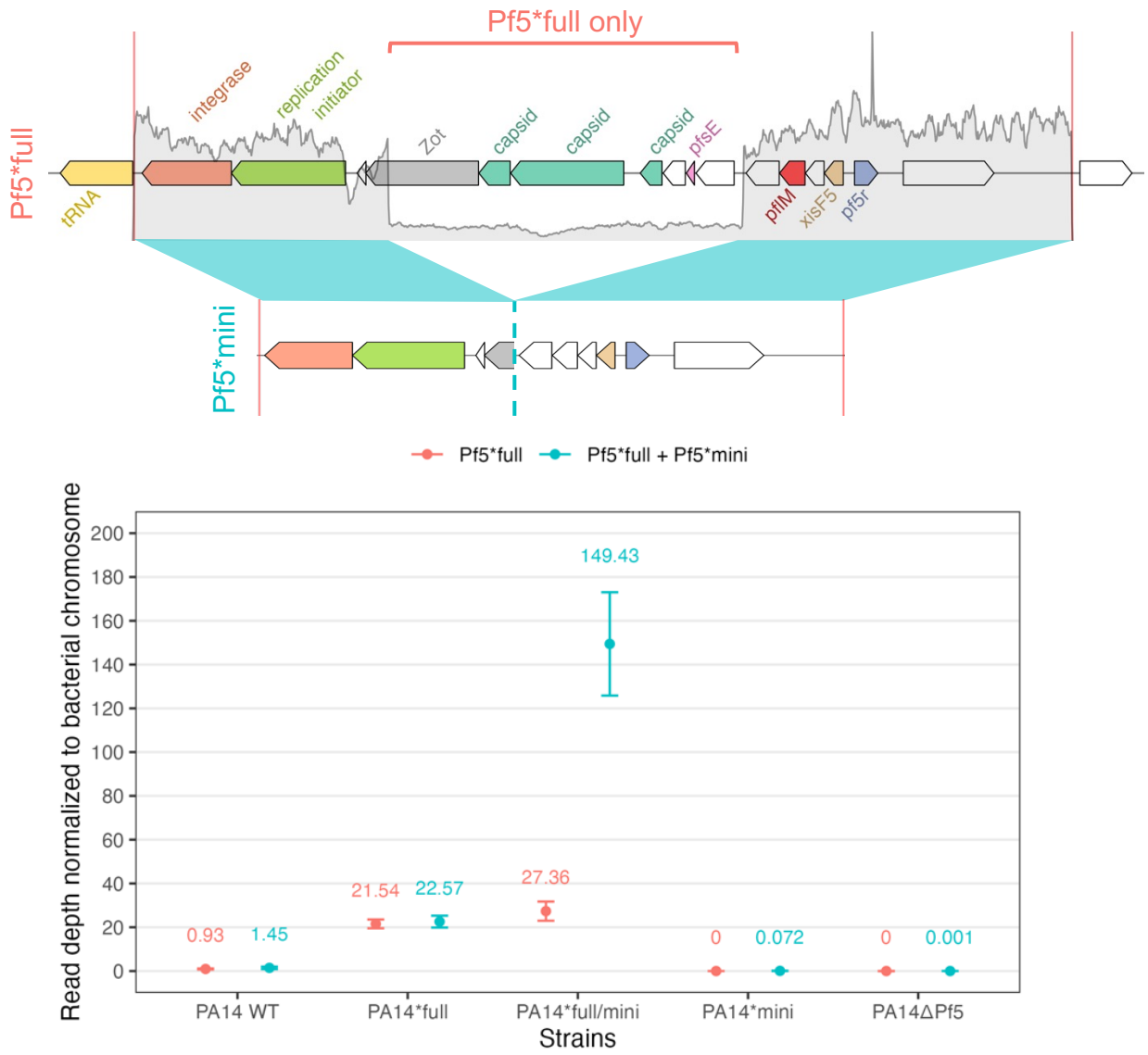

Supplemental figure 2. Read depths of the phage genome normalized to the bacterial chromosome show that the phage copy number increases when *pf5r* is mutated and increases again when both Pf5*full and Pf5*mini are present. Read depth was measured in 10 bp increments, and then they were normalized before calculating for the mean and standard deviation for each Pf5 region.

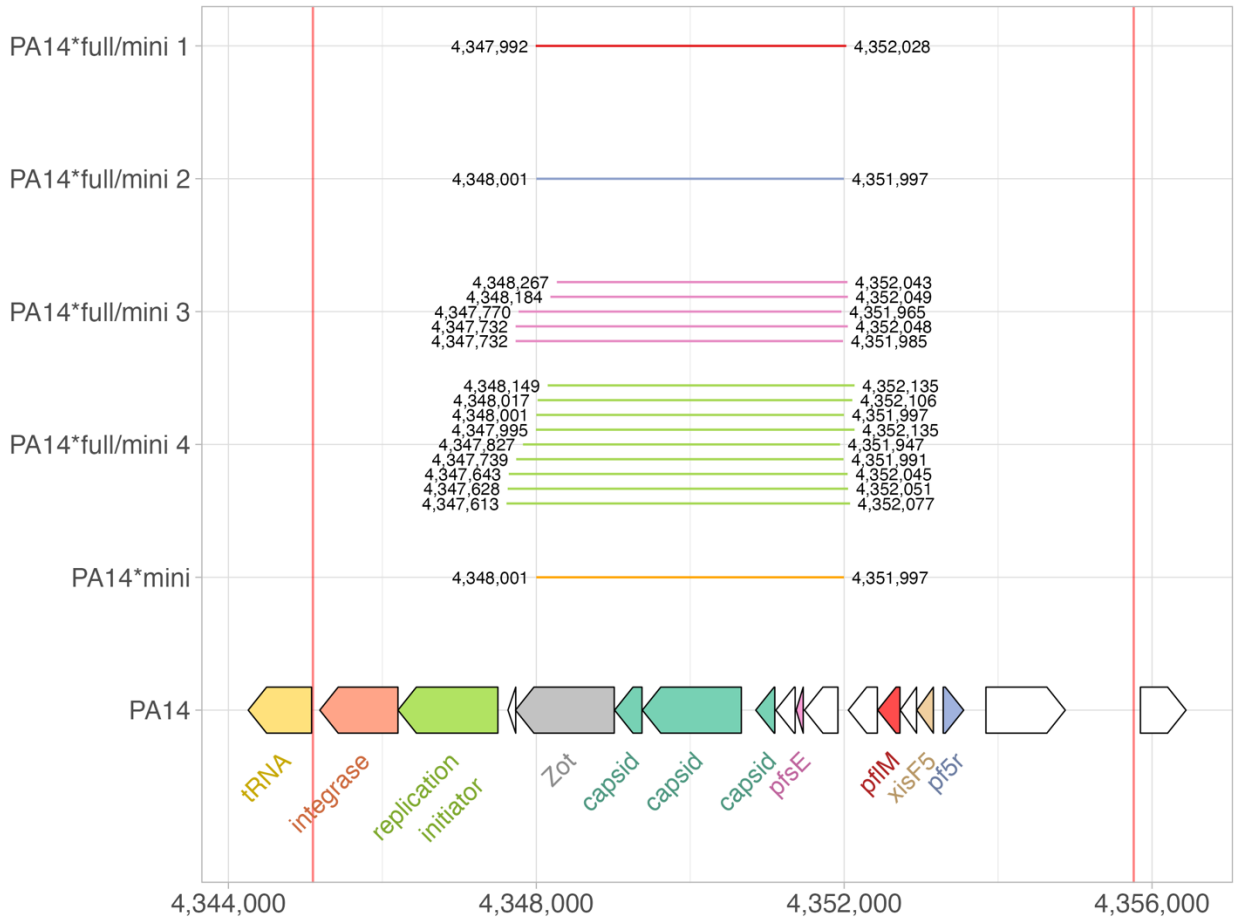

Supplemental figure 3. Miniphage emergence occurs independently multiple times following *pf5r* mutation. Five bacterial clones carrying miniphage(s) were isolated, and the horizontal lines denote the deletion edges of each clone's miniphage population. Some clones (i.e. PA14*full/mini 3&4) carry multiple miniphage genotypes while others only have one (i.e. PA14*full/mini 1&2 and PA14*mini). Deletion edges vary in their exact position but are consistently in the same region, with all indicating loss of structural genes like capsid.

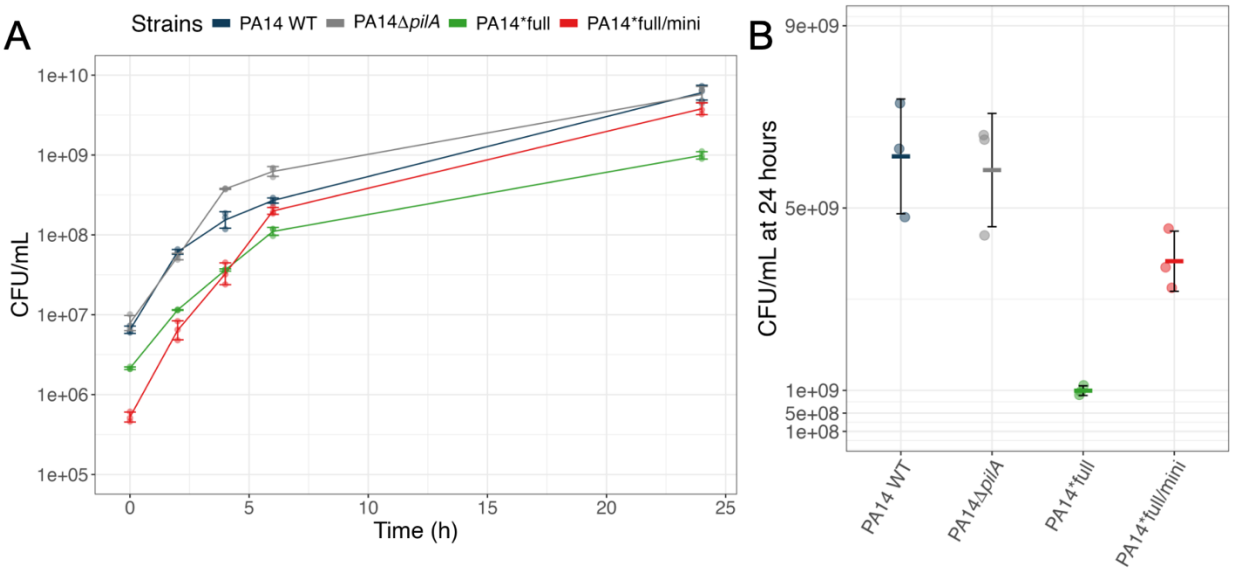

Supplemental figure 4. CFU/mL measurements of the bacteria correlate with the OD_{600} readings from Figure 2. (A) Timecourse CFU/mL of each strain and (B) CFU/mL comparison at 24 hours.